Journal of ELECTRONIC MATERIALS, Vol. 45, No. 3, 2016
DOI: 10.1007/s11664-015-4201-y

Cost Scaling of a Real-World Exhaust Waste Heat Recovery Thermoelectric Generator: A Deeper Dive

TERRY J. HENDRICKS,[1,4] SHANNON YEE,[2] and SANIYA LEBLANC[3]

1.—Power and Sensors Section, Thermal Energy Conversion Group, NASA-Jet Propulsion Laboratory, California Institute of Technology, 4800 Oak Grove Drive, Pasadena, CA 91109, USA. 2.—G. W. W. School of Mechanical Engineering, Georgia Institute of Technology, Atlanta, GA 30332, USA. 3.—Department of Mechanical & Aerospace Engineering, George Washington University, Washington, DC 20052, USA. 4.—e-mail: terry.j.hendricks@jpl.nasa.gov

Cost is equally important to power density or efficiency for the adoption of waste heat recovery thermoelectric generators (TEG) in many transportation and industrial energy recovery applications. In many cases, the system design that minimizes cost (e.g., the $/W value) can be very different than the design that maximizes the system's efficiency or power density, and it is important to understand the relationship between those designs to optimize TEG performance-cost compromises. Expanding on recent cost analysis work and using more detailed system modeling, an enhanced cost scaling analysis of a waste heat recovery TEG with more detailed, coupled treatment of the heat exchangers has been performed. In this analysis, the effect of the heat lost to the environment and updated relationships between the hot-side and cold-side conductances that maximize power output are considered. This coupled thermal and thermoelectric (TE) treatment of the exhaust waste heat recovery TEG yields modified cost scaling and design optimization equations, which are now strongly dependent on the heat leakage fraction, exhaust mass flow rate, and heat exchanger effectiveness. This work shows that heat exchanger costs most often dominate the overall TE system costs, that it is extremely difficult to escape this regime, and in order to achieve TE system costs of $1/W it is necessary to achieve heat exchanger costs of $1/(W/K). Minimum TE system costs per watt generally coincide with maximum power points, but preferred TE design regimes are identified where there is little cost penalty for moving into regions of higher efficiency and slightly lower power outputs. These regimes are closely tied to previously identified low cost design regimes. This work shows that the optimum fill factor F_{opt} minimizing system costs decreases as heat losses increase, and increases as exhaust mass flow rate and heat exchanger effectiveness increase. These findings have profound implications on the design and operation of various TE waste heat recovery systems. This work highlights the importance of heat exchanger costs on the overall TEG system costs, quantifies the possible TEG performance-cost domain space based on heat exchanger effects, and provides a focus for future system research and development efforts.

Key words: Thermoelectric systems, cost analysis, cost scaling, energy recovery, waste heat recovery

List of symbols

Variables

A	Total heat exchanger area (m^2)
A_{TE}	One n-type + p-type TE element area, TE couple area (m^2)
C''	TE material area-dependent manufacturing costs ($/$m^2$)
C'''	TE material volumetric-dependent costs ($/$m^3$)

(Received July 8, 2015; accepted October 30, 2015; published online November 25, 2015)

$C_{HX,C}$ Cold heat exchanger cost coefficient [$/(W/K)]
$C_{HX,H}$ Hot heat exchanger cost coefficient [$/(W/K)]
C_p Exhaust flow specific heat (J/kg K)
F TEG fill factor
F_{opt} Optimum TEG fill factor
G TE system total cost per output power ($/W)
I Electrical current (A)
k Thermal conductivity of TE material (W/m K)
K_C TE system cold-side conductance (W/K)
K_{exh} Exhaust conductance (= $\dot{m}C_p\varepsilon$) (W/K)
K_H Effective hot-side conductance (W/K)
K_{HX} Additional hot-side thermal conductance (W/K)
K_{TE} TE module thermal conductance (W/K)
$K_{\|}$ Parallel leakage thermal conductance (W/K)
L_{TE} TE element length (m)
$\dot{m}$ Mass flow rate of exhaust (kg/s)
N Number of TE couples
P TE power output (W)
Q Heat input from exhaust (W)
Q_C Heat rejected (W)
Q_H TE hot-side thermal input (W)
Q_{loss} Parasitic thermal loss at heat exchanger/TE interfaces (W)
$Q_{\|}$ Parallel leakage heat (W)
R TE module electrical resistance (Ω)
S_{pn} Junction seebeck coefficient (= $S_p - S_n$) (V/K)
T_1 TE hot-side junction temperature (K)
T_2 TE cold-side junction temperature (= T_{cold}) (K)
T_C Cold sink temperature (K)
T_{exh} Hot source (exhaust) temperature (K)
T_H Hot heat exchanger temperature (K)
T_m Mean junction temperature $(T_1 + T_2)/2$ (K)
U Overall heat exchanger heat transfer coefficient (W/m^2 K)
UA_h Overall hot-side heat exchanger conductance (W/K)
Z^* Optimum thermoelectric module figure of merit [= $S_{pn}^2/(R^*K_{TE})$] (1/K)

Greek letters

ε Heat exchanger effectiveness
η_{Total} Total TE system efficiency
η_{TE} TE module efficiency
ρ Material electrical resistivity [= $(\rho_p + \rho_n)/2$] (Ω m)
σ Heat loss fraction (= Q_{loss}/Q)

INTRODUCTION

Various commercial and military vehicles and industrial process systems create and dissipate enormous amounts of waste thermal energy globally every year. Various research and development projects have designed and developed advanced thermoelectric (TE) materials and systems to recover thermal energy in high-temperature transportation, industrial, and military energy systems. Thermoelectric generators (TEGs) for high-temperature, waste heat recovery applications have benefitted from significant TE materials advancements in these projects. The advancements enable TEGs with power output capabilities on the order ~100–1000 kW/m^2 and system-level efficiency of >7%. The barrier to commercial TEG applications lies in optimizing system cost, which should be approximately $1/W[1] to be competitive with currently used power technologies to foster market penetration.* Hence, system designs based on cost minimization are particularly useful. Comprehensive and integrated TE system performance and cost modeling is an absolute requirement for optimizing energy recovery systems, but little work has been done with this coupled modeling. Consequently, there are misconceptions and little quantifiable metrics to guide TE system designs in overcoming the system cost barriers.

Previous work investigated the material, manufacturing, and system component costs for TEG designs optimized for minimum system cost.[1,2] The work presented here utilizes the cost-performance metrics and applies them to realistic application scenarios using detailed TEG system models based on extensive prior work.[3–5] Notably, the analysis employs key, realistic system parameters by including heat lost to the environment from the exhaust source, heat exchanger effectiveness, exhaust mass flow rate effects, temperature-dependent TE properties (for skutterudite materials), and multiple exhaust and cold-side temperatures. The impact of current, realistic heat exchanger costs and target costs are investigated and quantified for common representative waste heat recovery conditions.

MATHEMATICAL FORMULATION

The mathematical framework that describes the thermal and electrical operation of a TEG is well established.[6] Recently, this framework was revisited in an exhaust waste-heat recovery scenario, which allowed a fraction of the heat to leak from the hot-side and cold-side heat exchangers.[3–5] More recently, cost-performance optimizations based on the aforementioned original mathematical framework were developed.[2] Herein, we demonstrate modifications to this cost-performance optimization in the scenario of exhaust waste heat recovery where a fraction of the heat is allowed to leak from the hot-side and heat exchanger performance is

*U.S. Department of Energy, Office of Energy Efficiency and Renewable Energy, Vehicle Technologies Program, Multi-year Program Plan, 2011–2015, December 2010; US Department of Energy, Sunshot Vision Study, 2012.

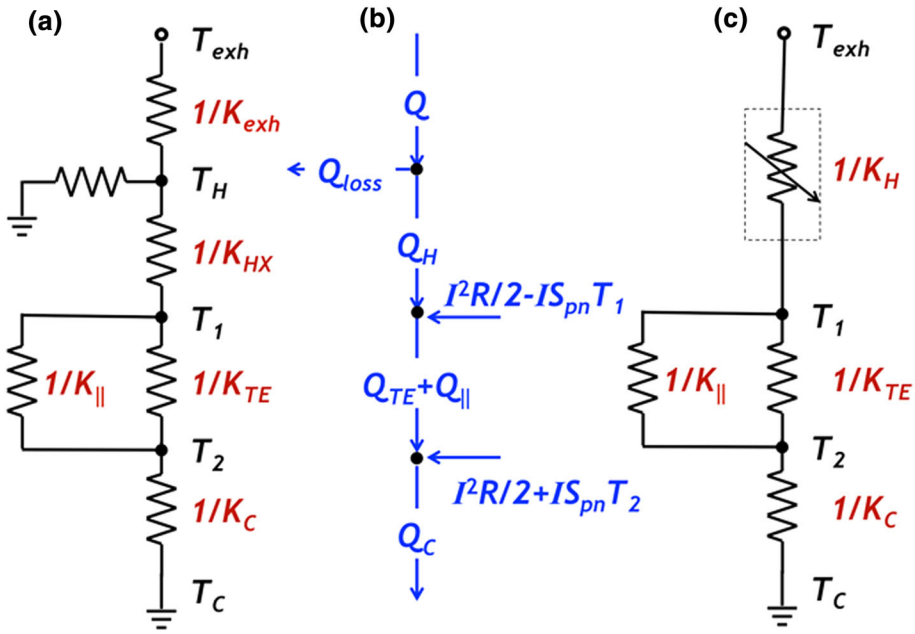

Fig. 1. (a) Thermal resistance network for exhaust waste-heat recovery including leakage from the hot-side heat exchanger. (b) Heat and electrical energy flows. (c) Equivalent (traditional) thermal circuit.

included. The thermal resistance network for this scenario is shown in Fig. 1a.

Using the ε-NTU methodology,[7] the thermal conductance corresponding to the exhaust heat exchanger can be expressed as a product of the heat exchanger effectiveness, ε, the exhaust flow specific heat, C_p, and the mass flow rate of exhaust, $\dot{m}$. In this methodology, heat from the exhaust is transferred to the hot-side heat exchanger, which is at intermediate temperature, T_H, before the heat is transferred to the TE module. It is also at this temperature that heat can be lost (*i.e.*, leaked to the cold-sink). The fraction of heat that is lost, σ, can be expressed as the ratio of that heat lost, Q_{loss}, to the heat delivered by the exhaust, Q. Performing an energy balance at the heat exchanger temperature node yields an expression for the heat entering the hot-side of the TE module, Q_H, which is similar to the expression given by Hendricks and Lustbader.[3,5,8]

$$Q_H = \frac{(T_{exh} - T_1)}{\left[\frac{1}{\dot{m}\cdot C_p\cdot\varepsilon\cdot(1-\sigma)} + \frac{1}{K_{HX}}\right]} \tag{1}$$

From this expression, one can define an effective hot-side conductance:

$$\frac{1}{K_H} = \frac{1}{\dot{m}\cdot C_p\cdot\varepsilon\cdot(1-\sigma)} + \frac{1}{K_{HX}} = \frac{K_{HX} + \dot{m}\cdot C_p\cdot\varepsilon\cdot(1-\sigma)}{\dot{m}\cdot C_p\cdot\varepsilon\cdot(1-\sigma)\cdot K_{HX}} \tag{2}$$

that simplifies the thermal resistance network in Fig. 1a into the more familiar (traditional) thermal resistance network in Fig. 1c. One can see that this effective hot-side conductance behaves like a variable thermal resistor whose value depends on the heat loss fraction, σ, mass flow rate of exhaust, $\dot{m}$, and heat exchanger effectiveness. This modification further propagates, and energy balances around the hot and cold junctions yield a system of non-linear equations that can be numerically evaluated to determine the exact junction temperatures.[1,2]

$$K_H(T_{exh} - T_1) - (K_{TE} + K_{||})(T_1 - T_2) - \frac{S_{pn}^2(T_1 - T_2)T_1}{2R} + \frac{S_{pn}^2(T_1 - T_2)^2}{8R} = 0 \tag{3a}$$

$$\frac{S_{pn}^2(T_1 - T_2)^2}{4R} - K_H(T_{exh} - T_1) + K_C(T_2 - T_C) = 0 \tag{3b}$$

These expressions are identical to those given by Yee[2] and LeBlanc[1] with minor modification of interpretation of the subscripts; the hot-side source temperature is now represented by T_{exh} and K_H is a variable conductance rather than a static conductance. Finally, Hendricks[4] showed that to maximize power output in a TEG waste heat recovery system, the cold-side conductance should be 10×–20× greater than the hot-side thermal conductance. Thus, for a fixed (static) hot-side conductance, there exists a maximum variable cold-side conductance that should be targeted to maximize power output. This analysis demonstrates the design impacts when hot-side heat exchanger thermal leakage, exhaust mass flow rate, and heat exchanger effectiveness are included.

To understand the cost-performance in this leaky, exhaust-waste-heat recover scenario, consider the total system cost normalized by the power output, P, given by Yee et al.[2] and LeBlanc et al.[1] The system cost ($/W) is given by:

$$G(\$/\mathrm{W}) = \frac{\text{Total TEG Costs}}{P} = \frac{\text{Total TEG Costs}}{\eta_{\mathrm{TE}} \cdot Q_{\mathrm{H}}} = \frac{\text{Total TEG Costs}}{\eta_{\mathrm{TE}} \cdot (1-\sigma) \cdot Q}, \quad (4)$$

and is directly related to the efficiency, η_{TE} (= P/Q_{H}), and either the heat entering the hot-side of the TE module, Q_{H} after leakage, or the total heat delivered including leakage, Q, given by Hendricks and Lustbader.[3–5] This thermal efficiency discounts thermal leakage from the hot-side heat exchanger and can be expressed as:

$$\eta_{\mathrm{TE}} = \frac{P}{Q_{\mathrm{H}}} = \left(\frac{T_1 - \mathrm{T}_2}{T_1}\right) \cdot \left(\frac{\sqrt{1+ZT_{\mathrm{m}}} - 1}{\sqrt{1+ZT_{\mathrm{m}}} - \frac{T_2}{T_1}}\right) \quad (5)$$

It is important to note that this expression for the efficiency is subject to the condition that the electrical load on the TEG is greater than the internal resistance of the TEG by a factor of $\sqrt{1+ZT_{\mathrm{m}}}$, which, to first-order, is the load that maximizes the efficiency of the TEG. It is also important to note that T_1 and T_2 are the junction temperatures, not the hot-source (exhaust) temperature, T_{exh}, or the cold-sink temperature, T_{sink}. Finally, we re-emphasize that this is the efficiency discounting thermal leakage and is a factor of $1/(1-\sigma)$ larger than the total system efficiency ($\eta_{\mathrm{Total}} = P/Q$).

The total TEG costs can be expressed as:

$$\text{Total TEG Costs}(\$) = (C''' \cdot L_{\mathrm{TE}} + C'') \cdot A \cdot F + C_{\mathrm{HX,H}} \cdot K_{\mathrm{H}} + C_{\mathrm{HX,C}} \cdot K_{\mathrm{C}}, \quad (6)$$

which is very similar to the expression provided by LeBlanc et al.[1] and Yee et al.,[2] but instead the heat exchanger cost coefficient and heat exchanger conductance for the hot and cold side are allowed to be different. However, since the heat exchanger cost coefficients are likely similar [*i.e.*, ~1–10 $/(W/K)], the cost will likely be dominated by the cold-side heat exchanger costs based on work by Hendricks.[4]

$$C_{\mathrm{HX,H}} \approx C_{\mathrm{HX,C}} \text{ and } K_{\mathrm{C}} \geq 20K_{\mathrm{H}}$$
$$\text{Total TEG Costs}(\$) \approx (C''' \cdot L_{\mathrm{TE}} + C'') \cdot A \cdot F + C_{\mathrm{HX,C}} \cdot K_{\mathrm{C}} \quad (7)$$

Furthermore, the total TEG costs are a function of the fill factor, F. It is important to remember that there is no fill factor that maximizes the efficiency or minimizes the cost. However, as given by Yee et al.,[2] there exists an optimum fill factor (defined by a point of diminishing returns) where reducing the fill factor below this value results in only a marginal reduction in the $/W cost. The optimum fill factor given by Yee et al.[2] is:

$$F_{\mathrm{opt}} \approx \frac{1}{2}\sqrt{\frac{C_{\mathrm{HX,H}} U_{\mathrm{H}}^2}{C'''k}} \quad (8)$$

Here the optimum fill factor is determined by the hot-side heat exchanger values as the limiting condition, because they are smaller than the cold-side heat exchanger values. This shows that the optimum fill factor is dependent on the thermal loss factor,σ, exhaust mass flow rate, and heat exchanger effectiveness through the hot-side heat exchanger heat transfer coefficient U_{H}. When heat is not lost,

$$\sigma \to 0 \quad (9)$$

a larger fill factor allows that heat to be effectively converted to power. Conversely, as more heat is lost, the device should be designed with smaller fill factors to allow for better-cost savings of the system.

Next, returning to Eq. 4, the cost-performance value G can be explicitly expressed as:

$$G = \frac{(C''' \cdot L_{\mathrm{TE}} + C'') \cdot A \cdot F + C_{\mathrm{HX,H}} \cdot K_{\mathrm{H}} + C_{\mathrm{HX,C}} \cdot K_{\mathrm{C}}}{(1-\sigma) \cdot \left(\frac{T_1 - T_2}{T_1}\right) \cdot \left(\frac{\sqrt{1+Z^*T_{\mathrm{m}}} - 1}{\sqrt{1+Z^*T_{\mathrm{m}}} + \frac{T_2}{T_1}}\right) \cdot K_{\mathrm{H}} \cdot (T_{\mathrm{exh}} - T_1)} \quad (10)$$

where $Z^* = S_{\mathrm{pn}}^2/(R^*K_{\mathrm{TE}})$. For the calculations that follow, we set $K_{\mathrm{C}} = 10\,K_{\mathrm{H}}$ where we employ this relationship between K_{C} and K_{H} developed by Hendricks[4] to maximize power output. Equation 10 gives one a first insight as to how real system heat losses affect system-level costs per watt, with increasing σ generally increasing system costs per watt by a factor on the order of $1/(1-\sigma)^2$, (*i.e.*, $\sim \partial G/\partial \sigma$). Therefore, while it has been intuitively and mathematically well known for years that minimizing system heat losses increases system performance, one can now also see that minimizing heat loss also minimizes system-level costs. In fact, cost per watt scaling directly with the non-dimensional factor $1/(1-\sigma)$ and cost per watt increasing as σ increases by $\sim \partial G/\partial \sigma$ shown above. In this work we generally set $\sigma = 0.1$ in order to demonstrate the lowest attainable costs of a real system, but emphasize that in real systems there may be higher heat losses that must be quantified. Furthermore, Eq. 10 also provides one insight into how cost per watt depends on heat exchanger mass flow rate and effectiveness implicitly via the K_{H} term through Eq. 2. However, cost per watt dependence on these two heat exchanger parameters is complex because K_{H} is in both the numerator (system cost) and denominator (power itself). Finally, for simplification we let $C_{\mathrm{HX,H}} = C_{\mathrm{HX,C}}$.

To further illustrate the cost-scaling, Eq. 10 can be reorganized into other non-dimensional groups to better illustrate the primary driving factors that

influence cost as done by Yee et al.[2] In this approach, it is necessary to define a characteristic thermal length:

$$L_T = \frac{k}{U_H}, \tag{11}$$

by which all the system lengths scale. Given this definition, by rearranging and unpacking $Z * T$ in Eq. 10, as done by Yee et al.,[2] this work recovers a modified cost-scaling factor:

$$G_o = \frac{16 \cdot C''' \cdot \rho \cdot L_T^2}{S_{pn}^2 \cdot (T_1 - T_2)^2} \tag{12}$$

This factor has units of \$/W and is simply a result of algebraic manipulation of Eq. 10 into a non-dimensional group (*e.g.*, G/G_0 is a non-dimensional group). This modified cost-scaling factor differs slightly from the one previously develop by Yee et al.,[2] in that it is a function of the junction temperatures and does not contain a simplification relating the junction temperatures to the reservoir temperatures, and in that the electrical resistivity is used instead of the electrical conductivity for cleanliness of notation in this document.

KEY PARAMETRIC SENSITIVITIES

Equations 10 and 12 show the mathematical relationship of what design parameters enter into the TEG system cost-per-watt analysis and how they affect the total calculation. Further in-depth analysis of the different design parameters and their relative magnitude of influence on overall costs reveals that TEG system costs are controlled by the following six parameters:

- T_{exh}
- T_2/T_1 (TE cold-side junction temperature to hot-side junction temperature ratio)
- TE module $Z * T$ (primarily the module thermal conductivity k, and separately the module power factor)
- K_H (and more importantly, K_C/K_H)
- C_{HX}
- σ

K_H and K_C strongly influence G, as they are the primary drivers for relating the reservoir temperatures to the junction temperatures. Furthermore, the exhaust temperature and the cold sink temperatures are also key sensitivity parameters; higher exhaust temperatures or lower cold-sink temperatures will always result in lower \$/W values scaling by Eq. 10. Therefore, waste heat recovery applications with these characteristics will benefit from this fundamental cost-scaling dependency. Finally, it is necessary to recognize that L_T is a function of the module's effective thermal conductivity k. Thus, the module $Z * T$ parameters strongly influence the cost scaling through L_T and the power factor recognized in Eq. 12. Because the controlling terms in Eq. 10 are the heat exchanger costs governed by $C_{HX,C}$ and $C_{HX,H}$, their values are critical in Eq. 10. Real-world TEG system applications are often constrained by potentially high heat exchanger costs, which must be controlled and minimized to make TEG systems more economically attractive.

Heat Exchanger Costs

LeBlanc et al.[1] and Yee et al.[2] have demonstrated that the cost of heat exchangers can be characterized by $C_{HX} * (UA)_{HX}$, such that higher heat exchanger conductance (UA) results in larger heat exchanger costs within Eqs. 6 and 7. However, the UA term is itself a combination of two heat exchanger attributes: U (W/m^2 K), the overall heat transfer coefficient that is described by Kays and London,[7] and A (m^2), the total exchanger heat transfer area. One generally pays for enhancements in either one or both of these terms, as summarized in Table I.

The costs of the various enhancements shown in Table I can impact the C_{HX} values one actually uses in any given application, and can ultimately affect or determine C_{HX} sensitivity. Earlier work by LeBlanc et al.[1] and Yee et al.[2] has shown that C_{HX} is often in the range of \$10/(W/K) to \$20/(W/K) for real-world heat exchangers. This work highlights this dependency in order to frame the ensuing discussions and guide future research and development work in bringing TEG systems to the forefront of energy recovery solutions.

COST ANALYSIS RESULTS AND DISCUSSION

Several system cost analyses were conducted for 773 K and 848 K hot-side exhaust temperatures, design parameters shown in Table II, and heat exchanger costs, generally focusing on a range of heat exchanger cost from \$1/(W/K) to \$10/(W/K). These analyses focused on using the latest TE material properties for skutterudite (SKD) materials, shown in Fig. 2,[9,10] developed by NASA-Jet Propulsion Laboratory (JPL) for advanced spacecraft power system applications, which are now available for transportation and industrial waste energy recovery applications. Exhaust temperatures of 773 K and 848 K are representative of engine exhaust and some industrial process heat recovery applications, respectively. Current heat exchanger costs are on the order of \$10/(W/K), while target costs are on the order of \$1/(W/K); an aggressive target requiring extensive future research and development investment to achieve. The key result is that TEG system costs are dominated by heat exchanger costs, even when heat exchanger cost is as low as \$1/(W/K). Figure 3 shows where these two important realistic heat exchanger cost cases reside on the dimensionless cost regime map developed by Yee et al.[2] This illustrates that it is extremely difficult in real-world

Table I. Heat exchanger attributes governing costs

Heat exchanger attribute	Enhancements that impact cost
U	Complex fin and flow geometries, microchannel designs, two-phase flow
A	Footprint area, volume, material selections

Table II. Design parameters used in predicting representative system performance and cost

C''' ($/m^3)	C''	F	TE element length (cm)	Exhaust mass flow, $\dot{m}$ (kg/s)	Heat loss factor, σ	UA_h (W/K)
8.66×10^{4}[11]	168.2[1,2]	0.2	0.25	0.1	0.1	200, 400

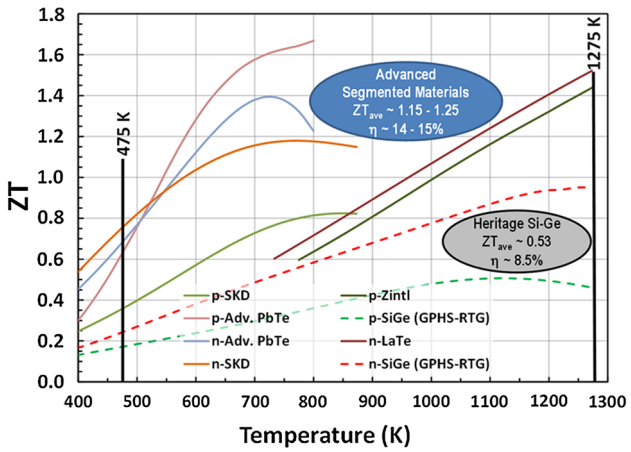

Fig. 2. Recent TE material advances for high-temperature, high-performance spacecraft power systems. Materials currently available for transportation and industrial waste energy recovery.[9,10]

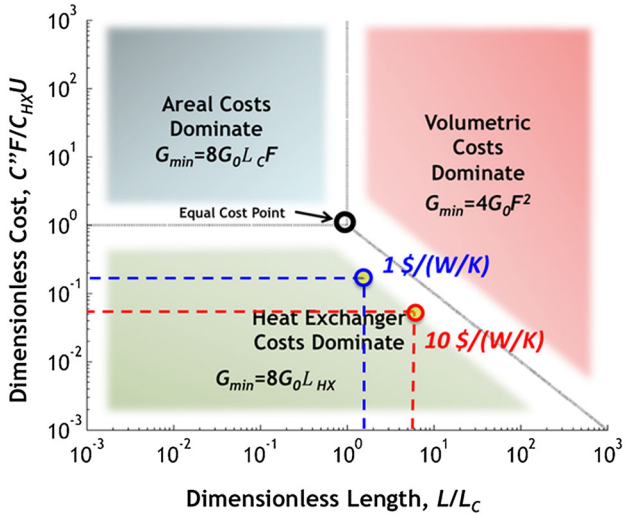

Fig. 3. Dimensionless cost versus dimensionless length showing regions where each cost component dominates. The two cases modeled here for realistic device and application parameters fall within the region where heat exchanger costs dominate.

TEG systems, which require crucial heat exchangers for high performance, to escape the heat exchanger dominated regime shown in Fig. 3.

The cost results demonstrate the controlling nature of the exhaust temperatures, where higher exhaust temperatures offer the opportunity to get more heat out of the system and lead to lower cost. The minimum TEG system cost varies by approximately 40% for the two exhaust temperatures. When the heat exchanger cost is \$1/(W/K), the minimum TEG costs are \$1.35/W and \$1.00/W for exhaust temperatures of 773 K (*e.g.*, engine exhaust applications) and 848 K (*e.g.*, industrial process applications), respectively, for design conditions in Table II. These minimum cost values are consistent in the cases of either maximum efficiency or maximum power. The minimum cost values are approximately one order of magnitude higher for heater exchanger costs of \$10/(W/K), since the TEG system cost is dominated by the heat exchanger cost.

The results for the best cost scenario (exhaust temperature of 848 K and heat exchanger cost of \$1/(W/K) are presented in Figs. 4, 5, 6, and 7 for three representative cold-side temperatures (333 K, 363 K, 398 K), and thus three ratios of hot to cold-side temperatures. These cold-side temperatures were generally selected to provide a reasonable, achievable range of cold-side temperatures to expose and quantify critical design sensitivities in Eq. 7. Figure 4 is simply the required TE material area (for a constant TE element length), and reflects how the (L_{TE}/A_{TE}) changes for different TE hot-side temperatures shown in Figs. 5 and 6. It shows how A_{TE} is changing for different thermal and power conditions, and its relationship to the maximum-power-point area requirement. Figure 5 shows the TE module efficiency versus power relationship and the well-known tradeoff between hot-side heat transfer into the system and TE conversion efficiency in defining the maximum power point[3–5] in this map. The performance benefits of operating in the "preferred TE design regime" are higher efficiency, higher power fluxes, and higher power density.[8] Figure 5 illustrates that when the temperature difference and temperature ratio are

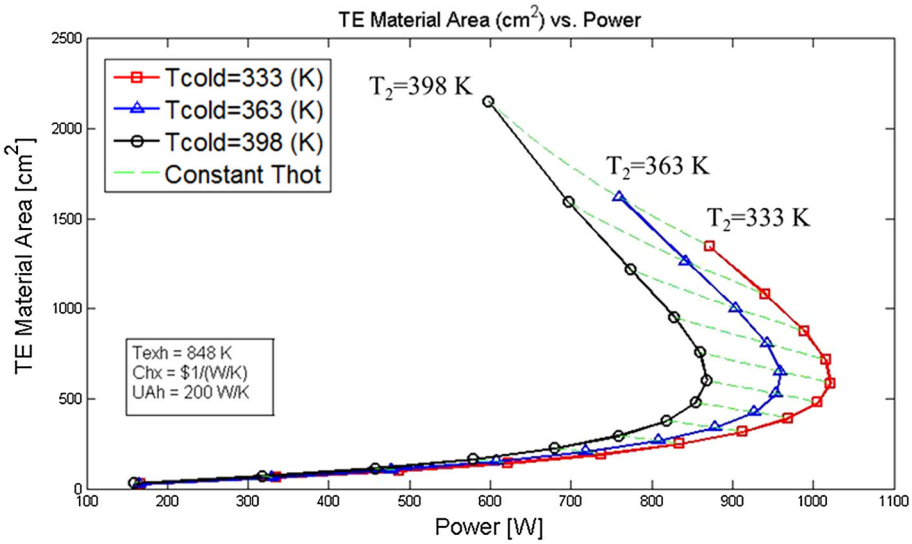

Fig. 4. Area of active thermoelectric material versus TEG power output for three cold-side temperatures [333 (red squares), 363 (blue triangles), 398 (black circles) K].

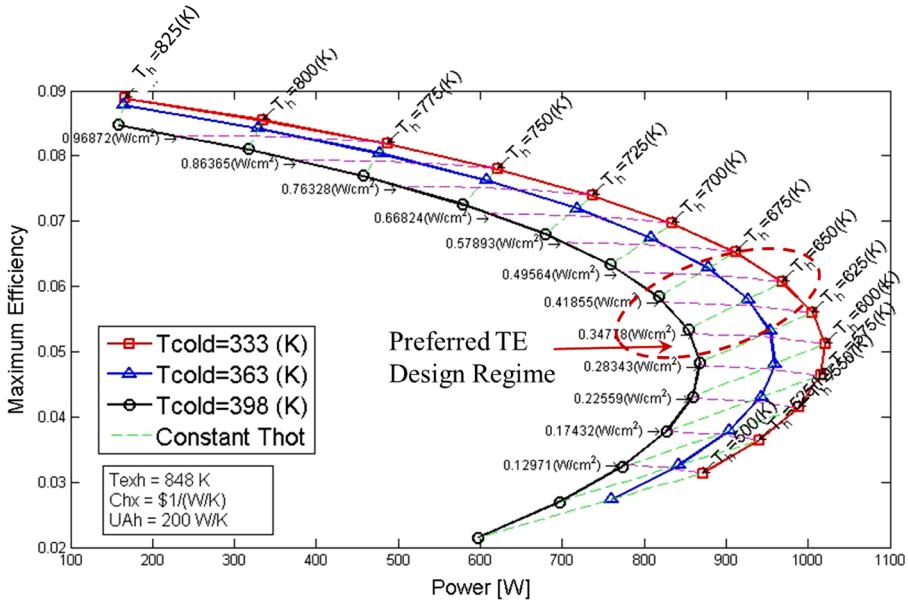

Fig. 5. Maximum system efficiency versus TEG power output for three cold-side temperatures.

largest (*i.e.*, cold-side temperature of 333 K), the maximum power generated increases dramatically to approximately 1020 W with a power flux of 0.35 W/cm^2 (3.5 kW/m^2) under these system analysis conditions. The TE module efficiency at the peak power point is approximately 5% with the *p*-type and *n*-type skutterudite materials in Fig. 2 at the hot-side and cold-side temperature levels shown in Fig. 5. In this chart, TE module efficiency can be related to overall total TE system efficiency through the relation:

$$\eta_{\text{Total}} = \frac{P \cdot (1 - \sigma)}{Q_{\text{H}}}. \tag{13}$$

Figures 5, 6, and 7 are used together to understand where power is maximizing and TEG system costs are minimizing in the possible design space for the cases analyzed, and how sensitive cost is to either the power or efficiency. Figures 6 and 7 represent the new information related to TE system costs from this work. Figure 6 shows how TE system costs vary with TE module efficiency and how those costs-per-watt minimize over a rather broad range of efficiencies, with system costs being relatively insensitive to efficiency over a broad range to either side of the minimum cost point. Because of this relationship, one can actually move into higher efficiency regimes

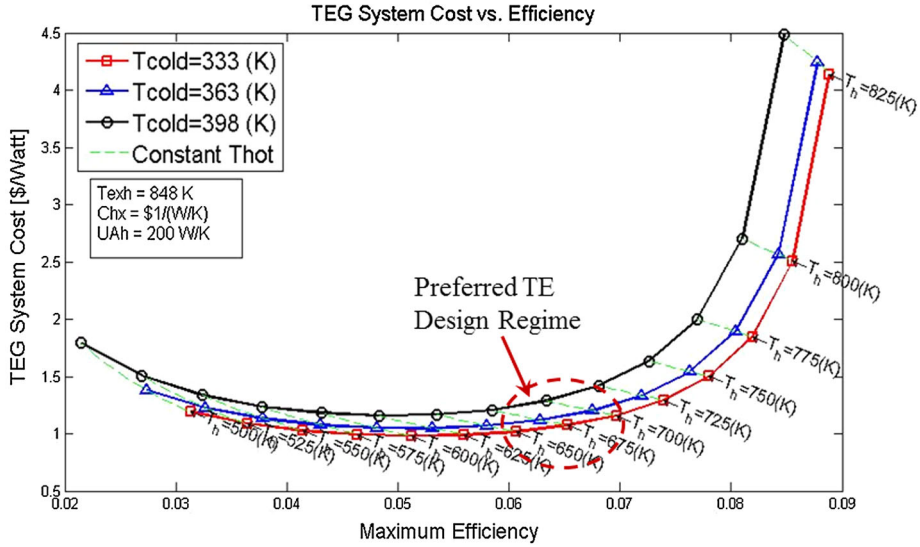

Fig. 6. Thermoelectric generator system cost in $/W versus maximum system efficiency for $1/(W/K) heat exchangers.

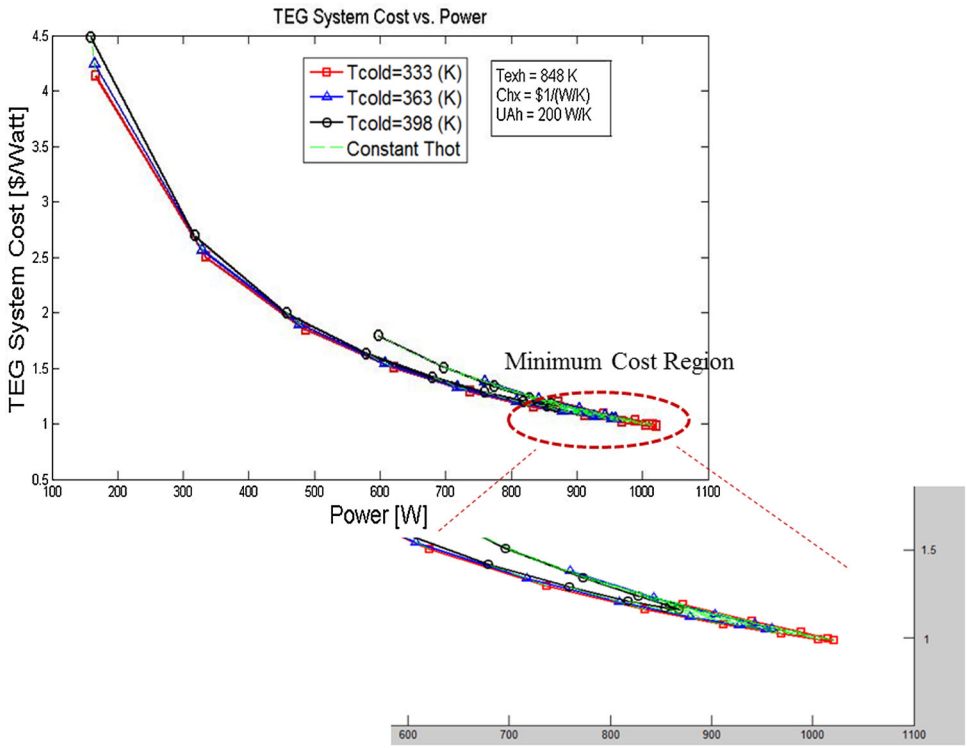

Fig. 7. Thermoelectric generator system cost in $/W versus power output for $1/(W/K) heat exchangers.

(*i.e.*, "preferred TE design regime") with very little system cost penalty. However, one does not want to go too far, as power decreases will eventually increase system costs-per-watt as illustrated in Fig. 6. It is noteworthy that the "preferred TE design regime" in Figs. 5 and 6 coincide and show the lack of significant cost penalty in this region, adding to already noted benefits of higher TE efficiency and higher TE system power density in this region.

The plots of TEG system cost versus power output (Fig. 7) and TEG system cost versus efficiency (Fig. 6) demonstrate the impact of the heat exchanger cost. It is clear in Figs. 6 and 7 that maximum power and minimum system cost points generally coincide and occur at a lower system cost for lower cold-side temperatures. Since the heat exchanger cost dominates the system cost, the system cost variation as a function of different cold-side temperatures is minimal around the minimum system cost regions shown in Figs. 6 and 7, characteristic of the asymptotic behavior discussed by Yee et al.[2] However, the system cost variation with cold-side

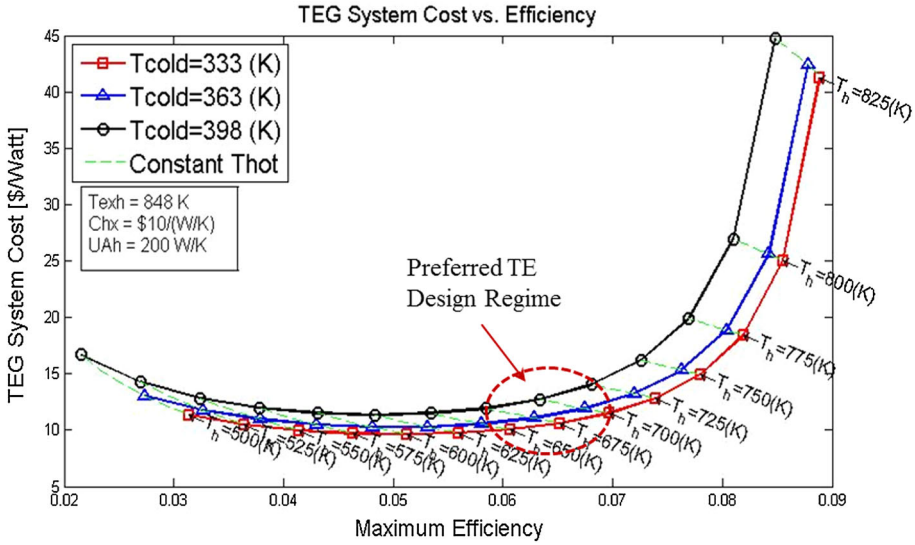

Fig. 8. Thermoelectric generator system cost in $/W versus maximum system efficiency for $10/(W/K) heat exchangers.

temperature grows as one moves away from this minimum system cost region. The dominance of the heat exchanger costs also collapses the cost relationship in Eq. 10 to one where essentially $G \sim 1/P$. If the heat exchanger cost did not dominate (*e.g.*, if instead the TE material cost dominated), then the curves for each cold-side temperature (or hot to cold-side temperature ratio) would separate out, and a stronger system cost variation with cold-side temperature would be more apparent. Higher power results in lower system cost, as illustrated by the point at which each curve reverses (*i.e.*, reaches its maximum power and minimum cost point); after that point, more TE material area and lower power results in higher system cost-per-watt. It is clear that lower cold-side temperatures can drive TEG system costs down, emanating from the $1/P$ relation as lower cold sides increase power. Therefore TEG system designers should strive to this goal for both cost and performance reasons in most waste heat recovery applications.

Additional system performance and cost analysis cases were performed for heat exchanger costs at $10/(W/K), with all other parameters in Table II held constant. The change in heat exchanger costs does not impact the results in Figs. 4 and 5. Figures 8 and 9 show the resulting TE system costs from Eq. 10 versus TE module efficiency and power output, respectively, for $10/(W/K) heat exchanger costs. Although the basic relationships remained similar to those in Figs. 6 and 7, it is clear that system costs generally increase by roughly the order of magnitude increase in heat exchanger costs. In this case, the TE system cost is even more dominated by the heat exchanger costs, as evidenced by the even tighter collapsing of the cost relationships in Fig. 9. Unfortunately, at this point in time, heat exchanger costs of ~$10/(W/K) are actually closer to reality and are the main driver as to why TE

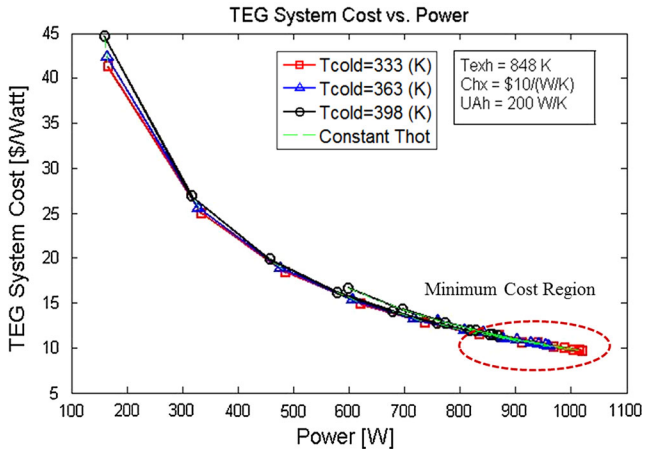

Fig. 9. Thermoelectric generator system cost in $/W versus power output for $10/(W/K) heat exchangers.

systems generally run ~$10/W in current applications. In order to significantly decrease the TE system costs and bring them down to ~$1/W, as desired by many organizations worldwide, this analysis clearly shows that research and development to reduce heat exchanger costs by an order of magnitude are required.

Additional system cost analyses were also performed to investigate the effect of lower T_{exh} and higher UA_h values. Higher UA_h values lead to higher K_H values through higher heat exchanger effectiveness given by Ref. 7:

$$\varepsilon = 1 - \exp\left(\frac{-UA_h}{\dot{m} \cdot C_p}\right) \tag{14}$$

and Eq. 2. Table III gives the resulting TE system cost-per-watt (*i.e.*, G) and maximum power for four different system performance cases shown. At both

Table III. Minimum TE system cost-per-watt point and maximum power as T_{exh} and UA_H vary—heat exchanger costs \$1/(W/K)

T_{exh}	773 K			848 K		
$T_2 = T_{cold}$	333 K	363 K	398 K	333 K	363 K	398 K
200 W/K	\$1.35/W 740 W	\$1.45/W 690 W	\$1.6/W 630 W	\$1/W 1020 W	\$1.07/W 960 W	\$1.2/W 870 W
400 W/K	\$1.35/W 850 W	\$1.45/W 795 W	\$1.6/W 730 W	\$1/W 1180 W	\$1.07/W 1110	\$1.2/W 1000 W

Multiply cost-per-watt values by 10× for heat exchanger costs of \$10/(W/K).

UA_H values shown, increasing T_{exh} from 773 K to 848 K decreases the system cost-per-watt significantly at each cold-side condition. This is a direct result of Eq. 10, where increasing T_{exh} in the final term of the denominator increases heat transfer into the TE system, therefore increasing power output and driving G lower. One can therefore see that waste energy recovery applications with higher T_{exh} conditions will necessarily have lower system costs.

In contrast, there is no effect on TE system costs per watt (*i.e., G*) from UA_H increasing from 200 W/K to 400 W/K at either T_{exh} condition for any cold-side condition. However, the power output increases dramatically as G stays constant when UA_H, and therefore K_H, increases. This is also a direct result of Eq. 10 for G. When the heat exchanger costs dominate in Eq. 10, K_C/K_H = 10–20, and K_H and $C_{HX,H}$ dominate the costs, then one reaches a point where the TEG costs in G (numerator of Eq. 10) become essentially proportional to K_H through $C_{HX,H}$. At that point, both the TEG costs (numerator) and the TEG power (denominator) in Eq. 10 are basically proportional to K_H and by examination the value and effect of K_H actually cancels out in Eq. 10; therefore, G mathematically becomes insensitive to K_H, and, in fact, UA_h as well through Eqs. 2 and 14.

The completely positive effect of minimizing T_{Cold} (= T_2) on both decreasing G and increasing power output is also evident in the data of Table III, once again driving home the design requirement to minimize cold-side temperature conditions in industrial or transportation waste energy recovery applications. This is a universal truth in waste energy recovery.

Fill Factor Dependence on Thermal Heat Losses, Exhaust Mass Flow Rates, Heat Exchanger Effectiveness

The fill factor has direct influence over the cost. In many applications, especially for waste-heat recovery applications, the fill factor is fixed by other system considerations, such as mechanical robustness or pick-and-place machine tolerances. However, if this parameter is allowed to be a free design variable in addition to the TE leg length, then the performance and cost of the TEG can be optimized differently.[2] To perform this optimization, one must consider the full free design domain and the resulting \$/W cost design space,[2] which is a function of both the fill factor and leg length. In this design space, there are two valleys; one that corresponds to the optimum fill factor for a fixed leg length, and another that corresponds to the optimum leg length for a fixed fill factor. These two valleys converge, and this is the location of the preferred design TE design regime[2,8] that minimizes the cost-per-watt value. This location is characterized by a fill factor given by Eq. 8 and by substituting Eq. 2 into Eq. 8, one can see the dependence of the fill factor to the heat loss and other thermal parameters.

$$F_{opt} \approx \frac{1}{2}\sqrt{\frac{C_{HX,H}}{C'''\cdot k}}\cdot\left(\frac{\dot{m}\cdot C_p\cdot\varepsilon\cdot(1-\sigma)\cdot K_{HX}}{K_{HX}\cdot A+\dot{m}\cdot C_p\cdot\varepsilon\cdot(1-\sigma)\cdot A}\right)$$
$$\Rightarrow \lim_{K_{HX}\gg\dot{m}\cdot C_p\cdot\varepsilon} F_{opt} \rightarrow \frac{1}{2}\sqrt{\frac{C_{HX,H}}{C'''\cdot k}}\cdot\left(\frac{\dot{m}\cdot C_p\cdot\varepsilon}{A}\right)\cdot(1-\sigma) \quad (15)$$

It is always desirable to maximize the interface conductance between the hot-side heat exchanger and the TE module; particularly into the regime where $K_{HX} \gg \dot{m}C_p\varepsilon$. Next, by Eq. 15, it is clear to see that the optimum fill factor is linearly related to heat loss fraction, and has a maximum value when the heat loss is minimum. Thus, as discussed earlier, with more heat loss, the device should be designed with smaller fill factors using less active material in order to minimize the \$/W system cost. It is also clear from Eq. 15 that the optimum fill factor is dependent on the exhaust mass flow rate, $\dot{m}$, and heat exchanger effectiveness, ε; the optimum fill factor increases in most design cases as either the exhaust flow rate or heat exchanger effectiveness increases. Hence, the optimum fill factor is inherently tied to the heat exchanger performance and exhaust mass flow rate in any given waste energy recovery application.

CONCLUSIONS

This work has expanded on the TE system cost analyses by LeBlanc et al.[1] and Yee et al.,[2] by incorporating the results of Hendricks[4] and then incorporating these into TE system level analyses

by Hendricks et al.[3,5,8] The effects of heat exchanger costs and performance have been accounted for in a new, expanded analysis, and have shown and quantified the critical importance of heat exchanger costs in TE system cost analysis. TE system costs are generally governed by:

- Waste energy exhaust temperature, T_{exh}
- TE cold-side junction temperature to hot-side junction temperature ratio, T_2/T_1
- TE module $Z * T$ (primarily the module thermal conductivity k, and separately the module power factor)
- Hot-side thermal conductance, K_H (and more importantly K_C/K_H)
- Heat exchanger cost factor, C_{HX} [$/(W/K)]
- Parasitic thermal losses, σ

In general, TE system costs, G ($/W) are dominated by heat exchanger costs everywhere in the range of $1/(W/K) to $10/(W/K) and above. It was discovered that to achieve a TE system cost of ~$1/W, it is necessary to achieve heat exchanger costs of ~$1/(W/K); an aggressive cost goal that would require significant research and development investment to achieve, since current costs are ~$10/(W/K) or higher. Minimum TE system costs generally occur at maximum power points, but not at maximum TE module or system efficiency or the highest power density. Increasing T_{exh}, decreasing T_2/T_1 and increasing $Z * T$ are all crucial to minimizing TE system costs-per-watt in all waste energy recovery applications. Therefore, energy recovery applications with higher T_{exh} benefit preferentially, and minimizing cold-side temperatures is required in all cases. Preferred TE design regimes have been identified where higher efficiency and higher power density are possible, with little TE system cost-per-watt penalty and little power loss penalty. These preferred TE design regimes coincide with the optimum cost regions identified by Yee et al.[2] This new work has demonstrated that the optimum fill factor, F_{opt}, minimizing TE system costs is dependent on parasitic thermal losses, exhaust mass flow rate, and heat exchanger effectiveness. Increasing exhaust mass flow rates and heat exchanger effectiveness increase F_{opt}, while increasing parasitic thermal losses decreases F_{opt}. This work highlights the critical importance of the heat exchanger costs and performance in optimizing TE system costs in transportation and industrial waste heat recovery applications worldwide.

ACKNOWLEDGEMENTS

This work was carried out under NASA Space Act Agreement No.43-17508, a contract between NASA and General Motors with funding from the U.S. Department of Energy, at the Jet Propulsion Laboratory, California Institute of Technology, under a contract to the National Aeronautics and Space Administration.

REFERENCES

1. S. LeBlanc, S.K. Yee, M.L. Scullin, C. Dames, and K.E. Goodson, *Renew. Sustain. Energy Rev.* 32, 313 (2014).
2. S.K. Yee, S. LeBlanc, K.E. Goodson, and C. Dames, *Energy Environ. Sci.* 6, 2561 (2013).
3. T.J. Hendricks and J. Lustbader, in *Proceedings of the 21st International Conference on Thermoelectrics* (Long Beach, CA: IEEE Catalogue #02TH8657, 2002), p. 381.
4. T.J. Hendricks, in *Proceedings, 1642, Materials Research Society,* mrsf13-1642-bb02-04 (2014). doi:10.1557/opl.2014.443.
5. T.J. Hendricks, *J. Energy Resour. Technol.* 129, 223 (2007).
6. S.W. Angrist, *Direct energy conversion*, 4, Chapter 4 ed. (Boston: Allyn and Bacon Inc., 1982), pp. 121–176.
7. W.M. Kays and A.L. London, *Compact heat exchangers*, 3, Chapter 2 ed. (New York: McGraw-Hill, 1984), pp. 11–78.
8. T.J. Hendricks and D. Crane, *Thermoelectric Energy Recovery Systems: Thermal, Thermoelectric and Structural Considerations" CRC Press Handbook of Thermoelectrics and its Energy Harvesting: Modules, Systems, and Applications in Energy Harvesting*, Book 2, Section 3, Chapter 22 (Boca Raton, FL: Taylor and Francis Group, 2012).
9. J.-P. Fleurial, S.K. Bux, B.C.-Y. Li, S. Firdosy, N.R. Keyawa, P.K. Gogna, D.J. King, J.M. Ma, K. Star, A. Zevalkink, and T. Caillat, in *Symposium BB: thermoelectric materials–from basic science to applications*, *Proceedings of 2013 Materials Research Society Fall Meeting*, Boston (2013).
10. S. Bux, J.-P. Fleurial, and T. Caillat, in *Proceedings of 11th International Energy Conversion Engineering Conference* (American Institute of Aeronautics and Astronautics, 2013).
11. J.-P. Fleurial and T. Caillat, *Internal Jet Propulsion Laboratory Thermoelectric Material Studies Based on Raw Material Suppliers* (Washington, DC: Thermal Energy Conversion Technology Group, National Aeronautics and Space Administration, 2010–2014).